Published in final edited form as:
Circ Res. 2013 August 2; 113(4): 365–371. doi:10.1161/CIRCRESAHA.113.301063.

Transgenic Mice for cGMP Imaging

Martin Thunemann[*], **Lai Wen**[*], **Matthias Hillenbrand**, **Angelos Vachaviolos**, **Susanne Feil**, **Thomas Ott**, **Xiaoxing Han**, **Dai Fukumura**, **Rakesh K. Jain**, **Michael Russwurm**, **Cor de Wit**, and **Robert Feil**

Interfakultäres Institut für Biochemie (M.T., L.W., M.H., A.V., S.F., R.F.) and IZKF-Transgene Tiere (T.O.), Universität Tübingen, Tübingen, Germany; Edwin L. Steele Laboratory for Tumor Biology, Department of Radiation Oncology, Massachusetts General Hospital and Harvard Medical School, Boston (X.H., D.F., R.K.J.); Institut für Pharmakologie und Toxikologie, Universität Bochum, Bochum, Germany (M.R.); and Institut für Physiologie, Universität zu Lübeck, Lübeck, Germany (C.d.W.)

Abstract

Rationale—Cyclic GMP (cGMP) is an important intracellular signaling molecule in the cardiovascular system, but its spatiotemporal dynamics in vivo is largely unknown.

Objective—To generate and characterize transgenic mice expressing the fluorescence resonance energy transfer–based ratiometric cGMP sensor, cGMP indicator with an EC_{50} of 500 nmol/L (cGi500), in cardiovascular tissues.

Methods and Results—Mouse lines with smooth muscle–specific or ubiquitous expression of cGi500 were generated by random transgenesis using an SM22α promoter fragment or by targeted integration of a Cre recombinase–activatable expression cassette driven by the cytomegalovirus early enhancer/chicken β-actin/β-globin promoter into the Rosa26 locus, respectively. Primary smooth muscle cells isolated from aorta, bladder, and colon of cGi500 mice showed strong sensor fluorescence. Basal cGMP concentrations were <100 nmol/L, whereas stimulation with cGMP-elevating agents such as 2-(N,N-diethylamino)-diazenolate-2-oxide diethylammonium salt (DEA/NO) or the natriuretic peptides, atrial natriuretic peptide, and C-type natriuretic peptide evoked fluorescence resonance energy transfer changes corresponding to cGMP peak concentrations of ≈3 μmol/L. However, different types of smooth muscle cells had different sensitivities of their cGMP responses to DEA/NO, atrial natriuretic peptide, and C-type natriuretic peptide. Robust nitric oxide–induced cGMP transients with peak concentrations of ≈1 to >3 μmol/L could also be monitored in blood vessels of the isolated retina and in the cremaster microcirculation of anesthetized mice. Moreover, with the use of a dorsal skinfold chamber model and multiphoton fluorescence resonance energy transfer microscopy, nitric oxide–stimulated vascular cGMP signals associated with vasodilation were detected in vivo in an acutely untouched preparation.

Conclusions—These cGi500 transgenic mice permit the visualization of cardiovascular cGMP signals in live cells, tissues, and mice under normal and pathological conditions or during pharmacotherapy with cGMP-elevating drugs.

Correspondence to: Robert Feil, PhD, Interfakultäres Institut für Biochemie, Universität Tübingen, Hoppe-Seyler-Strase 4, 72076 Tübingen, Germany. robert.feil@uni-tuebingen.de.
[*]These authors contributed equally.

The online-only Data Supplement is available with this article at http://circres.ahajournals.org/lookup/suppl/doi:10.1161/CIRCRESAHA.113.301063/-/DC1.

Keywords

biosensing techniques; cyclic GMP; fluorescence resonance energy transfer; microscopy, fluorescence, multiphoton; muscle, smooth; vasodilation

The second messenger, cyclic GMP (cGMP), controls cardiovascular, neuronal, and other physiological functions.[1–4] It is generated from GTP by guanylyl cyclases, which are stimulated by various signaling molecules and hormones such as nitric oxide (NO) and natriuretic peptides.[5] It is degraded to GMP by phosphodiesterases, which are themselves often regulated by cGMP or cyclic AMP.[6] cGMP can also be excreted by transport proteins located in the plasma membrane.[7] Dysfunctions of the cGMP signaling cascade have been linked to a number of disorders such as retinal degeneration,[8] Alzheimer disease,[9,10] metabolic syndrome,[11] and arterial hypertension.[11,12] Drugs that increase the intracellular cGMP concentration are successfully used in the clinics, for instance, organic nitrates for the treatment of angina pectoris or the phosphodiesterase-5 inhibitor sildenafil (Viagra) for erectile dysfunction and pulmonary hypertension. However, the mechanisms that underlie the multiple roles of cGMP in (patho-)physiology and therapy are not fully understood, in part because it is difficult to monitor cGMP signals in live cells or tissues. Protein-based fluorescent biosensors are powerful tools for real-time imaging of cGMP in native cells.[13,14] In this study, we have generated and characterized, to the best of our knowledge for the first time, transgenic mouse lines that express a cGMP indicator.

Methods

Transgenic cGMP sensor mice were generated by random or targeted transgenesis in oocytes or embryonic stem cells, respectively. Epifluorescence fluorescence resonance energy transfer (FRET) microscopy was used to monitor intracellular cGMP in primary cells and tissues isolated from sensor mice and in the cremaster microcirculation of anesthetized sensor mice. cGMP in blood vessels of the skin was imaged in dorsal skinfold chambers by multiphoton FRET microscopy. For details on mouse generation, cell isolation, cGMP measurements by FRET microscopy and ELISA, expression analysis by reverse-transcription polymerase chain reaction, and statistics, an expanded Methods section is available in the Online Data Supplement.

Results

Generation of cGi500 Transgenic Mice

To generate transgenic cGMP sensor mice, we have used the recently developed, improved sensor cGMP indicator with an EC_{50} of 500 nmol/L (cGi500), which displays fast binding kinetics and exquisite selectivity for cGMP over cyclic AMP.[15] It consists of the tandem cGMP-binding domains of the cGMP-dependent protein kinase type I flanked by cyan fluorescent protein (CFP) and yellow fluorescent protein (YFP). The detection of cGMP is based on a decrease of FRET from CFP to YFP on binding of cGMP (Figure 1A). Transgenic cGi500 mice were generated by the following 2 strategies: (1) random integration of an expression cassette driven by a 445-bp fragment of the smooth muscle–specific SM22α promoter (SM22-cGi500 mice; Online Figure IA) and (2) targeted knock-in into the Rosa26 locus of a Cre recombinase–activatable expression cassette driven by the ubiquitous cytomegalovirus early enhancer/chicken β-actin/β-globin (CAG) promoter (R26-CAG-cGi500 mice; Online Figure II). Note that the R26-CAG-cGi500(L1) mouse line that we describe here carries the permanently activated sensor transgene (designated L1 allele in Online Figure IIA).

Western blot analysis of tissues from SM22-cGi500 mice with an anti–enhanced green fluorescent protein antibody demonstrated expression of the sensor in smooth muscle–rich tissues such as aorta, bladder, and colon but not in skeletal muscle or other nonsmooth muscle tissues (Online Figure IB and data not shown). Expression of the sensor in bladder and colon was unexpected because the SM22α-445 promoter fragment that was used in our transgene was originally reported not to be active in visceral smooth muscle.[16] The cGi500 protein detected in lysates of the bladder and colon by Western blotting (Online Figure IB) might have been derived from vascular smooth muscle. However, whole-mount preparations analyzed by fluorescence microscopy confirmed that the sensor was indeed expressed in bladder and colon smooth muscle (Online Figure IC). Differences in the expression pattern of SM22α-445 promoter–driven transgenes may be attributable to different chromosomal integration sites in different transgenic mouse lines. Primary smooth muscle cells isolated from the aortic vasculature, bladder, and colon (vasculature smooth muscle cells [VSMCs], bladder smooth muscle cells [BSMCs], and colon smooth muscle cells [CSMCs], respectively) of SM22-cGi500 mice showed strong fluorescence of the sensor in ≈25% of the cells, indicating robust but mosaic expression of the transgene (Online Figure ID). At the single-cell level, the fluorescence was distributed homogeneously in the cytoplasm without nuclear localization. On the basis of the analysis of sensor fluorescence, the R26-CAG-cGi500(L1) mice showed widespread and uniform cGi500 expression in most organs and tissues of adult mice (Online Figure IIIA), in embryos (Online Figure IIIB), and in primary cells derived from them (Online Figure IIIC and IIID and data not shown). The cGi500 transgenic mice were apparently healthy and fertile and had a normal life expectancy. Neither of the 2 mouse lines showed signs of toxicity of sensor expression. The mean arterial blood pressure of SM22-cGi500 mice as measured by the tail cuff method was not significantly different from that of nontransgenic control littermates (84±2 mm Hg [n=5] versus 78±5 mm Hg [n=4]).

cGMP Imaging in Primary Smooth Muscle Cells

To validate the new cGi500 transgenic mice for cGMP imaging, we monitored FRET changes in smooth muscle because it is one of the best-characterized target tissues of cGMP and smooth muscle relaxation is a classic function of cGMP.[17–19] First, we analyzed primary VSMCs isolated from SM22-cGi500 mice by using an epifluorescence-based FRET imaging setup. The cells were superfused for 2 minutes with C-type natriuretic peptide (CNP) or with the NO-releasing compound 2-(N,N-diethylamino)-diazenolate-2-oxide diethylammonium salt (DEA/NO), which activate guanylyl cyclases at the plasma membrane or in the cytosol, respectively. Both stimuli induced rapid and reversible changes of the CFP and YFP emissions in opposite directions, indicative of a change in FRET efficiency after binding of cGMP to the sensor protein (Figure 1B and 1C, cyan and yellow). Thus, the resulting increases in the CFP/YFP emission ratio should reflect CNP- and NO-induced cGMP signals (Figure 1B, right; Figure 1C, black trace). Similar results were obtained with VSMCs of R26-CAG-cGi500(L1) mice (Online Figure IV). To estimate intracellular cGMP concentrations from our FRET data, we used a calibration curve of the cGi500 sensor that was recorded in escin-permeabilized VSMCs with our epifluorescence imaging setup.[20] According to this in-cell calibration and in agreement with data determined for cGi500 in-cell extracts with a fluorescence spectrometer,[15] the cGi500 sensor has a dynamic range of cGMP detection of ≈100 nmol/L to 3 μmol/L and an EC_{50} value of 577 nmol/L. On the basis of these calibration data, the basal cGMP concentration in the primary VSMCs was below the detection limit of ≈100 nmol/L of the indicator, whereas stimulation with 50 nmol/L CNP or 100 nmol/L DEA/NO resulted in peak concentrations of ≈3 μmol/L cGMP (Figure 1C). These cGMP concentrations are well in the range over which cGMP receptors are activated, and they are consistent with previous reports, suggesting that maximal cGMP concentrations of 2 to 4 μmol/L may be physiological in smooth muscle.[21]

To test whether the cGMP concentrations determined by FRET imaging of cGi500-expressing cells correlate with measurements of cGMP levels by an independent assay, we compared FRET-derived data with results obtained with a cGMP ELISA. VSMCs, BSMCs, or CSMCs were stimulated for 2 minutes with 200 nmol/L DEA/NO. FRET imaging indicated that all 3 cell types responded with transient cGMP elevations (Figure 2, bottom). For cGMP ELISAs, aliquots of the cells were lysed shortly before the application of DEA/NO, 2 minutes after the application of DEA/NO, and 3 minutes after removal of DEA/NO (Figure 2, top). In general, the cGMP changes measured by FRET and ELISA correlated well with each other. We also attempted to calculate absolute intracellular cGMP concentrations from the ELISA data on the basis of the number of cells in each sample and an average cell volume of 1.0 pL.[22] The ELISA-derived cGMP concentrations that were in the dynamic detection range of the cGi500 sensor (≈100 nmol/L to 3 μmol/L; Figure 2, top, hatched rectangle) were indeed comparable to FRET-derived values. For example, the cGMP concentration in BSMCs at the end of the DEA/NO application (data point at 12 minutes in Figure 2) measured by both FRET and ELISA was ≈1 μmol/L. These results with primary smooth muscle cells confirm and extend the data of Russwurm et al,[15] showing a good correlation of cGMP signals measured by radioimmunoassay and FRET-based cGi sensors in HEK-293 cells. We conclude that FRET imaging of cGi500-expressing cells allows the measurement of intracellular cGMP concentrations between 100 nmol/L and 3 μmol/L in live cells in real time.

A detailed characterization of cGMP signals in VSMCs, BSMCs, and CSMCs revealed differences between these smooth muscle types. Dose-response experiments (Figure 3A) showed that all 3 cell types responded well to NO, but with different sensitivities, in the following order: BSMCs>VSMCs>CSMCs (corresponding EC_{50} for DEA/NO=73 nmol/L, 106 nmol/L, 147 nmol/L). The molecular basis of their differential sensitivity to NO is not clear but might reflect different equipment of each smooth muscle cell type with guanylyl cyclases and phosphodiesterases. Semiquantitative reverse-transcription polymerase chain reaction analysis indicated that VSMCs, BSMCs, and CSMCs express similar mRNA levels for the α^1 and β^1 subunits of NO-responsive soluble guanylyl cyclase (Online Figure V). Preincubation with the nonspecific phosphodiesterase inhibitor 3-isobutyl-1-methylxanthine strongly potentiated NO-induced cGMP signals in all cell types (Figure 3B). The relatively selective phosphodiesterase-5 inhibitor sildenafil had a comparatively weaker effect on all 3 cell types (Figure 3C). We conclude that cGMP levels in VSMCs, BSMCs, and CSMCs are controlled by phosphodiesterase-5 and other phosphodiesterases; the latter might at least in part contribute to the differential sensitivity of these cell types to NO. Further experiments indicated that these smooth muscle cell types also respond differentially to atrial natriuretic peptide (ANP) and CNP (Figure 3D). VSMCs showed relatively weak, but clearly detectable, cGMP signals on stimulation with ANP and robust signals on stimulation with CNP; BSMCs did not respond to ANP but responded to CNP to a similar extent as VSMCs; CSMCs were not responsive to ANP or CNP. In line with these results, mRNA for the ANP receptor guanylyl cyclase-A was detected only in VSMCs, and mRNA for the CNP receptor guanylyl cyclase-B was detected in VSMCs and BSMCs (Online Figure V). Surprisingly, mRNA for guanylyl cyclase-B was also expressed in CSMCs (Online Figure V), which, however, did not increase cGMP levels on incubation with CNP (Figure 3D). Elucidation of this discrepancy requires further investigations.

Detection of Vascular cGMP Signals in Isolated Tissues and Living Mice

Next, we analyzed cGMP signals in VSMCs of blood vessels in acutely isolated retinae of SM22-cGi500 mice. As expected, these vessels showed mosaic sensor fluorescence (Figure 4A). Nevertheless, on superfusion of DEA/NO, we recorded pronounced cGMP transients in these vessels (Figure 4B). The peak concentrations of cGMP were ≈1 μmol/L. To validate

the cGi500 mice in vivo, we performed intravital FRET microscopy of small arteries in anesthetized mice. These studies were done with R26-CAG-cGi500(L1) mice, which exhibit stronger and more homogeneous cGi500 expression in small vessels than SM22-cGi500 mice. At first, the microcirculation was studied in the cremaster muscle because these arterioles are amenable to intravital microscopy and exhibit a functional NO/cGMP pathway leading to vasodilation.[23] FRET imaging was performed with an epifluorescence setup similar to that used for the analysis of primary cells and isolated retinae. As illustrated in Figure 5 and in Online Movie I, robust and reversible cGMP signals were detected in arterioles on repeated superfusion of the tissue with DEA/NO. The cGMP transients reached peak concentrations of >3 μmol/L. Adenosine, a vasoactive substance that is thought not to affect cGMP levels, was applied as a negative control.

As a second in vivo model of vascular cGMP imaging, we used multiphoton FRET imaging of blood vessels in cGi500 mice carrying a dorsal skinfold chamber.[24] To induce cGMP increases, anesthetized animals received intravenous injections of DEA/NO. This model allows long-term noninvasive and more physiological imaging than the cremaster preparation, in which the tissue is acutely exposed and superfused with DEA/NO. Sensor fluorescence was clearly detectable in the vasculature of the skin (Figure 6A and 6C). Repeated injection of 100 μL DEA/NO (1 mmol/L) resulted in clear increases of the FRET ratio signal recorded in the vessel wall, indicating NO-induced vascular cGMP signals (Figure 6B). The cGMP concentration began to increase shortly (≈5–10 seconds) after DEA/NO injection (Figure 6 and data not shown). The DEA/ NO-stimulated increases of the FRET ratio were derived from characteristic changes of the CFP and YFP emissions in opposite directions, and injection of 100 μL vehicle (saline) did not induce such changes (Figure 6B). Moreover, the profiles of the cGMP transients correlated with the dose of DEA/ NO and with the extent of vessel relaxation (Figure 6D). The NO-induced vasodilations are also presented in a time-lapse video (Online Movie II). Note that the video was recorded in the CFP channel and thus shows sensor fluorescence but not FRET ratio signals. Interestingly, multiple injections of the lower dose of DEA/NO (0.1 mmol/L) resulted in desensitization of both the cGMP and the vasorelaxation response, whereas the higher dose of DEA/NO (1 mmol/L) evoked sustained responses that could not be further increased by another injection of the drug (Figure 6D).

Discussion

In this study, we have generated and characterized transgenic mice expressing the FRET-based cGMP indicator cGi500. Our results indicate that the cGi500 transgenic mice permit the visualization of cardiovascular cGMP signals in real time in live cells. Importantly, cGMP sensor mice are useful tools to study vascular cGMP signals associated with vasodilation in vivo. However, these experiments have also limitations. First, the maximal NO-induced changes of the FRET ratio signal that were recorded with the multiphoton microscope were ≈5% (Figure 6) as compared with ≈30% with the epifluorescence setup (eg, Figure 5). However, without calibration of the sensor under the conditions of multiphoton imaging, it is not clear whether the lower ratio changes reflect lower cGMP concentrations or physical differences between the imaging setups. Second, it is difficult to estimate the plasma concentrations of NO that induced cGMP elevations in vivo. The doses of the prodrug DEA/NO that were injected into the tail vein in these experiments seem relatively high (100 μL of a 0.1- or 1-mmol/L solution). However, if we assume that NO is released from 100 μL of a 0.1-mmol/L DEA/NO solution during a period of 5 to 10 seconds (half-life of DEA/NO, 2.1 minutes at pH 7.4 and 37°C; 1.5 moles NO per 1 mole of DEA/ NO),[25] the total blood volume of an adult mouse is 1.5 mL, and 95% of the released NO is bound to hemoglobin in erythrocytes,[26] then the concentration of free NO that evoked

cGMP transients (Figure 6D) was roughly 15 to 30 nmol/L, which is presumably in the range of physiological NO concentrations.[27]

Taken together, our results show that cGMP can be readily detected in smooth muscle cells of SM22-cGi500 and R26-CAG-cGi500(L1) mice, both in vitro and in vivo, opening new experimental routes for studying cGMP signaling in smooth muscle. For instance, primary cells isolated from cGi500 transgenic mice could be used to analyze subcellular cGMP compartments.[28] Because these cells express the cGMP sensor throughout the cytoplasm, global cGMP in the cytosol can be visualized by epifluorescence microscopy, whereas local cGMP pools at the plasma membrane can be imaged by confocal microscopy or total internal reflection fluorescence microscopy.[29,30] Another exciting application of the cGi500 mice is the characterization of NO- or natriuretic peptide–induced cGMP responses in different vascular beds in vivo. Because of its strong and uniform sensor expression, the R26-CAG-cGi500(L1) mouse line might be better suited for most in vivo applications, but the sparser and specific labeling of smooth muscle cells in the SM22-cGi500 mouse line allows better imaging of individual cells, which are difficult to delineate in the ubiquitous line. In addition, the widespread sensor expression in R26-CAG-cGi500(L1) mice will be useful for real-time monitoring of cGMP signals in many other tissues and cell types under normal and pathological conditions; these mice might also be a valuable tool to identify target tissues of old and new cGMP-elevating drugs. Note that we have also generated a R26-CAG-cGi500(L2) mouse line that carries a loxP-silenced cGi500 transgene (designated L2 allele in Online Figure II). In the basal state, cells of this mouse line express a red fluorescent protein from the L2 allele, but Cre-mediated recombination converts the L2 into the L1 allele (Online Figure II). Recombined cells carrying the L1 allele express the cGi500 sensor and can be used for cGMP imaging (Online Figure VI). Crossbreeding the R26-CAG-cGi500(L2) mouse line with tissue-specific Cre mice allows cGi500 expression to be selectively switched on only in tissues or cell types of interest. Thus, these new cGi500 transgenic mouse lines, which will be made available to the scientific community, provide multiple imaging options to study the mechanisms of cGMP signaling and to discover new sites of cGMP action in vivo in mammals.

Supplementary Material

Refer to Web version on PubMed Central for supplementary material.

Acknowledgments

We thank Barbara Birk and Julia Kahn for excellent technical assistance and Kübra Gülmez, Saskia Kroll, Moritz Lehners, Phillip Messer, Annyesha Mohanty, Kjestine Schmidt, Christine Wenz, and Ayline Wilhelm for their contributions to the generation and characterization of the cGi500 transgenic mice. Special thanks go to Eric N. Olson for the SM445 promoter fragment, Ralf Kühn for the ROSA26 probe, Liqun Luo for the pRosa26-mT/mG plasmid, and Mario Gimona for the SM22α antibody, as well as Jan Deussing, Thomas Münch, and the members of the Feil laboratory for advice and discussion.

Sources of Funding

This work was supported by grants from the Deutsche Forschungsgemeinschaft.

Nonstandard Abbreviations and Acronyms

ANP	atrial natriuretic peptide
BSMC	bladder smooth muscle cell
CAG	cytomegalovirus early enhancer/chicken β-actin/rabbit β-globin

CFP	cyan fluorescent protein
cGi500	cGMP indicator with an EC_{50} of 500 nmol/L
cGMP	cyclic GMP
CNP	C-type natriuretic peptide
CSMC	colon smooth muscle cell
DEA/NO	2-(N,N-diethylamino)-diazenolate-2-oxide diethylammonium salt
FRET	fluorescence resonance energy transfer
VSMC	vascular smooth muscle cell from aorta
YFP	yellow fluorescent protein

References

1. Beavo JA, Brunton LL. Cyclic nucleotide research: still expanding after half a century. Nat Rev Mol Cell Biol. 2002; 3:710–718.
2. Kemp-Harper B, Feil R. Meeting report: cGMP matters. Sci Signal. 2008; 1:pe12.
3. Kleppisch T, Feil R. cGMP signalling in the mammalian brain: role in synaptic plasticity and behaviour. Handb Exp Pharmacol. 2009; 191:549–579.
4. Tsai EJ, Kass DA. Cyclic GMP signaling in cardiovascular pathophysiology and therapeutics. Pharmacol Ther. 2009; 122:216–238.
5. Potter LR. Guanylyl cyclase structure, function and regulation. Cell Signal. 2011; 23:1921–1926.
6. Francis SH, Blount MA, Corbin JD. Mammalian cyclic nucleotide phosphodiesterases: molecular mechanisms and physiological functions. Physiol Rev. 2011; 91:651–690.
7. Sager G. Cyclic GMP transporters. Neurochem Int. 2004; 45:865–873. [PubMed: 15312981]
8. Trifunović D, Sahaboglu A, Kaur J, Mencl S, Zrenner E, Ueffing M, Arango-Gonzalez B, Paquet-Durand F. Neuroprotective strategies for the treatment of inherited photoreceptor degeneration. Curr Mol Med. 2012; 12:598–612.
9. Calabrese V, Mancuso C, Calvani M, Rizzarelli E, Butterfield DA, Stella AM. Nitric oxide in the central nervous system: neuroprotection versus neurotoxicity. Nat Rev Neurosci. 2007; 8:766–775.
10. Menniti FS, Faraci WS, Schmidt CJ. Phosphodiesterases in the CNS: targets for drug development. Nat Rev Drug Discov. 2006; 5:660–670. [PubMed: 16883304]
11. Martel G, Hamet P, Tremblay J. Central role of guanylyl cyclase in natriuretic peptide signaling in hypertension and metabolic syndrome. Mol Cell Biochem. 2010; 334:53–65. [PubMed: 19937369]
12. Ehret GB, Munroe PB, Rice KM, et al. Genetic variants in novel pathways influence blood pressure and cardiovascular disease risk. Nature. 2011; 478:103–109. [PubMed: 21909115]
13. Honda A, Sawyer CL, Cawley SM, Dostmann WR. Cygnets: in vivo characterization of novel cGMP indicators and in vivo imaging of intracellular cGMP. Methods Mol Biol. 2005; 307:27–43. [PubMed: 15988053]
14. Nikolaev VO, Lohse MJ. Novel techniques for real-time monitoring of cGMP in living cells. Handb Exp Pharmacol. 2009; 191:229–243. [PubMed: 19089332]
15. Russwurm M, Mullershausen F, Friebe A, Jäger R, Russwurm C, Koesling D. Design of fluorescence resonance energy transfer (FRET)-based cGMP indicators: a systematic approach. Biochem J. 2007; 407:69–77. [PubMed: 17516914]
16. Li L, Miano JM, Mercer B, Olson EN. Expression of the SM22alpha promoter in transgenic mice provides evidence for distinct transcriptional regulatory programs in vascular and visceral smooth muscle cells. J Cell Biol. 1996; 132:849–859. [PubMed: 8603917]
17. Carvajal JA, Germain AM, Huidobro-Toro JP, Weiner CP. Molecular mechanism of cGMP-mediated smooth muscle relaxation. J Cell Physiol. 2000; 184:409–420. [PubMed: 10911373]

18. Lincoln TM, Dey N, Sellak H. Invited review: cGMP-dependent protein kinase signaling mechanisms in smooth muscle: from the regulation of tone to gene expression. J Appl Physiol. 2001; 91:1421–1430. [PubMed: 11509544]
19. Nakatsu K, Diamond J. Role of cGMP in relaxation of vascular and other smooth muscle. Can J Physiol Pharmacol. 1989; 67:251–262. [PubMed: 2547502]
20. Thunemann M, Fomin N, Krawutschke C, Russwurm M, Feil R. Visualization of cGMP with cGi biosensors. Methods Mol Biol. 2013; 1020:89–120. [PubMed: 23709028]
21. Matchkov VV, Aalkjaer C, Nilsson H. A cyclic GMP-dependent calcium-activated chloride current in smooth-muscle cells from rat mesenteric resistance arteries. J Gen Physiol. 2004; 123:121–134. [PubMed: 14718479]
22. Hevia D, Rodriguez-Garcia A, Alonso-Gervós M, Quirós-González I, Cimadevilla HM, Gómez-Cordovés C, Sainz RM, Mayo JC. Cell volume and geometric parameters determination in living cells using confocal microscopy and 3D reconstruction. Protocol Exchange. 2011 Dec 8. http://www.nature.com/protocolexchange/protocols/2264.
23. Koeppen M, Feil R, Siegl D, Feil S, Hofmann F, Pohl U, de Wit C. cGMP-dependent protein kinase mediates NO- but not acetylcholine-induced dilations in resistance vessels in vivo. Hypertension. 2004; 44:952–955. [PubMed: 15505114]
24. Brown E, Munn LL, Fukumura D, Jain RK. In vivo imaging of tumors. Cold Spring Harb Protoc. 2010; 2010 pdb.prot5452.
25. Maragos CM, Morley D, Wink DA, Dunams TM, Saavedra JE, Hoffman A, Bove AA, Isaac L, Hrabie JA, Keefer LK. Complexes of NO with nucleophiles as agents for the controlled biological release of nitric oxide: vasorelaxant effects. J Med Chem. 1991; 34:3242–3247. [PubMed: 1956043]
26. Lancaster JR Jr. Simulation of the diffusion and reaction of endogenously produced nitric oxide. Proc Natl Acad Sci USA. 1994; 91:8137–8141. [PubMed: 8058769]
27. Hall CN, Garthwaite J. What is the real physiological NO concentration in vivo? Nitric Oxide. 2009; 21:92–103. [PubMed: 19602444]
28. Fischmeister R, Castro LR, Abi-Gerges A, Rochais F, Jurevicius J, Leroy J, Vandecasteele G. Compartmentation of cyclic nucleotide signaling in the heart: the role of cyclic nucleotide phosphodiesterases. Circ Res. 2006; 99:816–828. [PubMed: 17038651]
29. Bierbower SM, Shapiro MS. Förster resonance energy transfer-based imaging at the cell surface of live cells. Methods Mol Biol. 2013; 998:209–216. [PubMed: 23529432]
30. Nausch LW, Ledoux J, Bonev AD, Nelson MT, Dostmann WR. Differential patterning of cGMP in vascular smooth muscle cells revealed by single GFP-linked biosensors. Proc Natl Acad Sci USA. 2008; 105:365–370. [PubMed: 18165313]

Novelty and Significance

What Is Known?

- The cyclic nucleotide cyclic GMP (cGMP) is an important second messenger that transmits signals from nitric oxide and natriuretic peptides.
- Drugs that increase the intracellular cGMP concentration are used for the treatment of erectile dysfunction and pulmonary hypertension.
- The physiological outcome of cGMP signal transduction may depend on the spatiotemporal profiles of the intracellular cGMP signals and the prevalence of global versus local cGMP pools.

What New Information Does This Article Contribute?

- Transgenic mouse lines were generated that express a cGMP indicator protein that changes its fluorescence upon binding of cGMP so that intracellular cGMP can be monitored and quantified in real time in live cells.
- These mouse models provide new opportunities to study cardiovascular cGMP signaling in vivo.

To improve our understanding of the physiological and pathophysiological functions of cGMP and to monitor its spatiotemporal dynamics in native systems, we generated transgenic mouse lines that express an improved cGMP indicator protein based on fluorescence resonance energy transfer. The new cGMP sensor mice were characterized for their use in cGMP imaging. Proof-of-principle experiments showed that cGMP can be visualized in primary cells and tissues isolated from these mice, and in live animals. In addition, we present new biological findings on differential cGMP signals in different types of smooth muscle cells. Because of the design of the transgene construct, expression of the cGMP indicator can be specifically targeted to any tissue or cell type of interest. We anticipate that the cGMP sensor mouse will become a useful tool for monitoring cGMP levels in vivo.

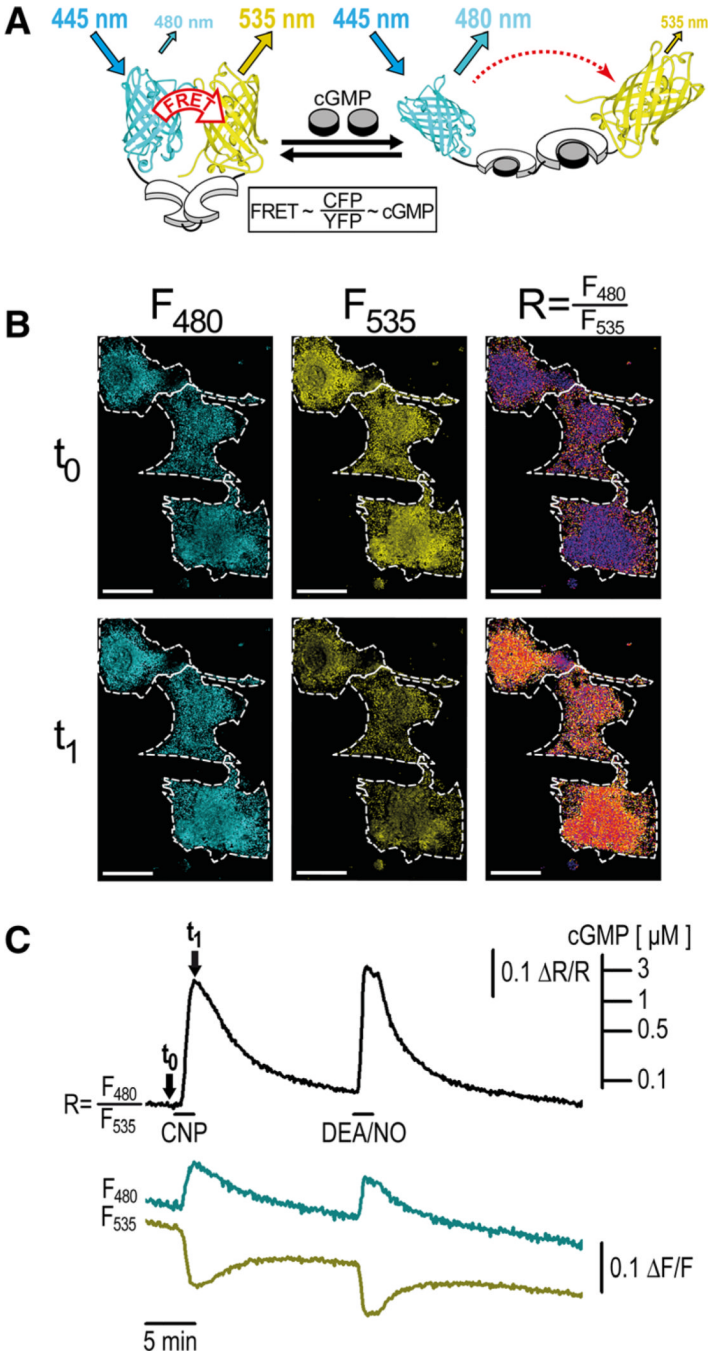

Figure 1. Cyclic GMP (cGMP) fluorescence resonance energy transfer (FRET) in primary vascular smooth muscle cells (VSMCs) from SM22-cGMP indicator with an EC_{50} of 500 nmol/L (cGi500) mice

A, Working principle of cGi500 sensor. This cGMP indicator consists of the tandem cGMP-binding sites of the bovine cGMP-dependent protein kinase type I (white) flanked by cyan fluorescent protein (CFP) and yellow fluorescent protein (YFP); its apparent EC_{50} value for cGMP is ≈500 nmol/L. In the absence of cGMP, FRET occurs from excited CFP to YFP, leading to light emission from YFP. Binding of cGMP (gray) causes a conformational change and a decrease in FRET efficiency. Thus, light emission from YFP at 535 nm is reduced, whereas emission from CFP at 480 nm is increased. The FRET efficiency of

cGi500 is depicted as the CFP/YFP emission ratio, which increases on cGMP binding to the biosensor. CFP and YFP structures are from the protein database (PDB-IDs: 2WSN and 3VD3). **B**, Compared with baseline (t_0), superfusion of primary VSMCs from SM22-cGi500 mice with 50 nmol/L C-type natriuretic peptide (CNP) leads to an increase of the CFP/YFP emission ratio, $R=F_{480}/F_{535}$ (t_1), which is a measure for the intracellular cGMP concentration. Cell borders are indicated by dashed lines. Scale bar, 20 μm. **C**, Brief stimulations (2 minutes) with CNP (50 nmol/L) or 2-(N,N-diethylamino)-diazenolate-2-oxide diethylammonium salt (DEA/NO; 100 nmol/L) lead to reversible cGMP increases. Cyan, yellow, and black traces indicate CFP emission (F_{480}), YFP emission (F_{535}), and the CFP/YFP emission ratio (F_{480}/F_{535}), respectively. Signals were recorded from the top left cell in **B**; the signals at time points, t_0 and t_1 correspond to the pictures shown in **B**. Emission intensities and ratios were normalized to averaged baseline signals and are given as ΔF/F and ΔR/R, respectively. The cGMP concentration scale bar was derived from in-cell calibration of the cGi500 sensor.[20]

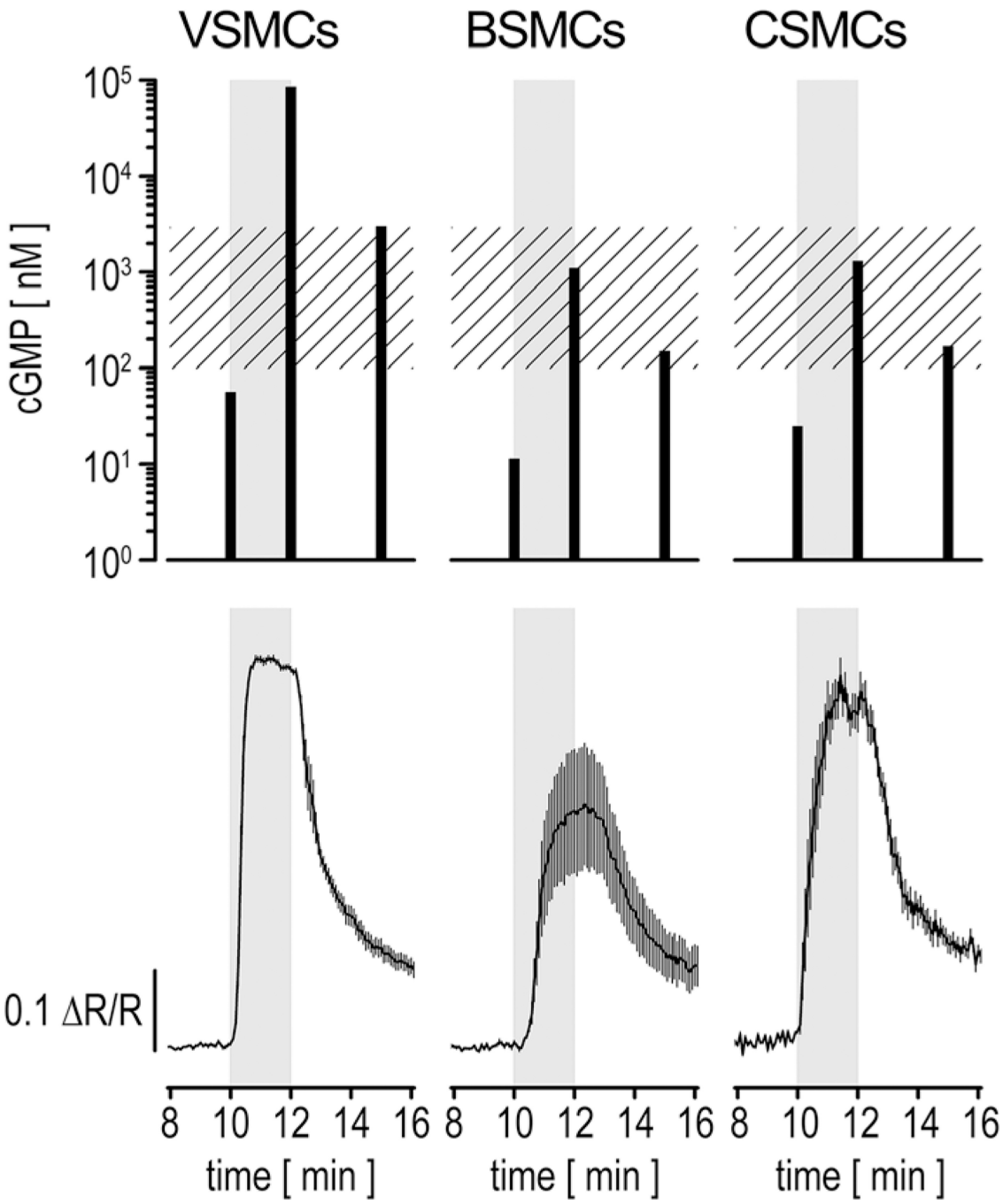

Figure 2. Comparison of nitric oxide (NO)–induced cyclic GMP (cGMP) changes measured by ELISA and fluorescence resonance energy transfer (FRET) imaging

Primary vascular smooth muscle cells (VSMCs), bladder smooth muscle cells (BSMCs), or colon smooth muscle cells (CSMCs) were stimulated for 2 minutes with 200 nmol/L 2-(N,N-diethylamino)-diazenolate-2-oxide diethylammonium salt (DEA/NO; gray rectangles). For ELISA measurements (**upper**), cell extracts were prepared shortly before (t=10 minutes), at the end of (t=12 minutes) the DEA/NO simulation, and 3 minutes after DEA/NO removal (t=15 minutes). For each time point, cells from 2 wells of a 6-well plate were pooled, and samples were measured in duplicate. Intracellular cGMP concentrations (black bars) were estimated from a cell number of 122 000 cells per measured sample and an

approximate cell volume of 1 pL.[22] Note that basal cGMP concentrations (t=10 minutes) for all cell types and the cGMP content in VSMCs at t=12 minutes represent extrapolations because the original readings were not within the calibration range of the ELISA. The hatched rectangle indicates the dynamic detection range of cGMP indicator with an EC_{50} of 500 nmol/L (cGi500) for cGMP. For FRET imaging (**bottom**), cells were grown and stimulated under conditions similar to the ELISA experiment. Cells were continuously superfused with buffer at 1 mL/min and stimulated with DEA/NO after 10 minutes. Images were acquired every 5 seconds. Averaged recordings of 5 VSMCs, 4 BSMCs, and 8 CSMCs are shown (mean±SEM). Cells for ELISA and FRET experiments were isolated from wild-type and R26-CAG-cGi500(L1) mice, respectively.

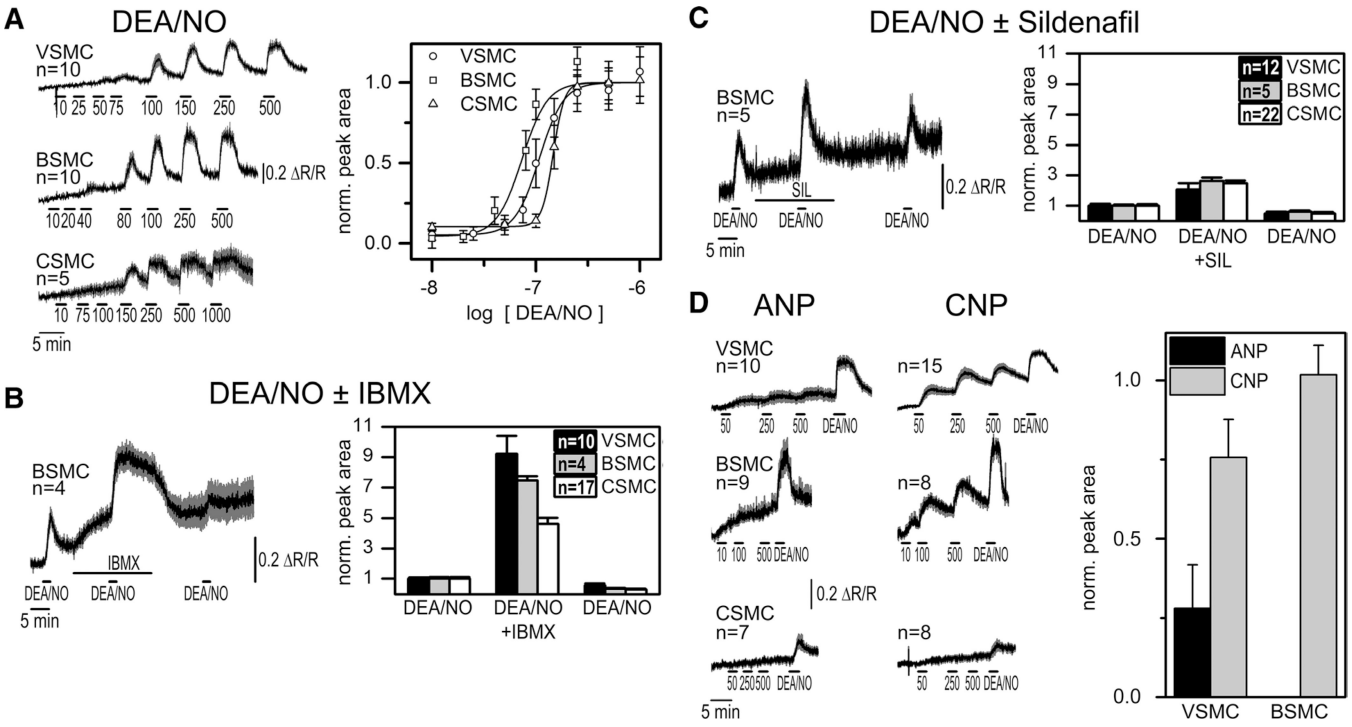

Figure 3. Characterization of cyclic GMP (cGMP) signals in different smooth muscle cell types (vascular smooth muscle cells [VSMCs], bladder smooth muscle cells [BSMCs], or colon smooth muscle cells [CSMCs]) isolated from SM22-cGMP indicator with an EC_{50} of 500 nmol/L (cGi500) mice

A, 2-(N,N-diethylamino)-diazenolate-2-oxide diethylammonium salt (DEA/NO)–cGMP dose-response experiments; original recordings (**left**) and estimated ΔR/R peak areas (**right**) upon stimulation for 2 minutes with increasing concentrations of DEA/NO (in nmol/L). For dose-response curves, data were normalized to the curve maximum. Curves are significantly different between BSMCs, VSMCs, and CSMCs ($P<0.01$ for all pairwise comparisons) with EC_{50} values (in nmol/L) of 73±8, 106±7, and 147±1, respectively. **B** and **C**, Phosphodiesterase inhibition with 3-isobutyl-1-methylxanthine (IBMX; **B**) or sildenafil (**C**) potentiates NO-induced cGMP responses. Cells were stimulated with a subsaturating concentration of DEA/NO deduced from dose-response curves in **A** (eg, VSMCs, 75 nmol/L; BSMCs, 50 nmol/L; CSMCs, 100 nmol/L) before, during, and after incubation with 300 μmol/L IBMX (**B**) or 30 μmol/L sildenafil (**C**). Representative original recordings are shown for BSMCs (**left**). A summary of NO-induced cGMP signals before, during, and after phosphodiesterase inhibition is shown in the bar diagrams. Peak areas were normalized to the first peak of each experiment. Note that in the case of IBMX treatment, the second peak area does not reflect real cGMP levels because the cGi500 sensor becomes saturated until IBMX is removed. **D**, Differential cGMP responses of VSMCs, BSMCs, and CSMCs to natriuretic peptides. Cells were superfused for 2 minutes with the indicated concentrations (in nmol/L) of atrial natriuretic peptide (ANP; **left**) or C-type natriuretic peptide (CNP; **right**). As a positive control, DEA/NO was applied at the end of each experiment (VSMCs, 500 nmol/L; BSMCs, 100 nmol/L; CSMCs, 500 nmol/L). The bar diagram summarizes the cGMP signals induced by 500 nmol/L ANP or CNP in VSMCs and BSMCs. The ΔR/R peak areas were normalized to the control stimulation with DEA/NO. Only VSMCs responded to ANP. All data are mean±SEM (n cells in the experiment as indicated in the respective panel). Representative results from ≥4 experiments with independent cell cultures are shown.

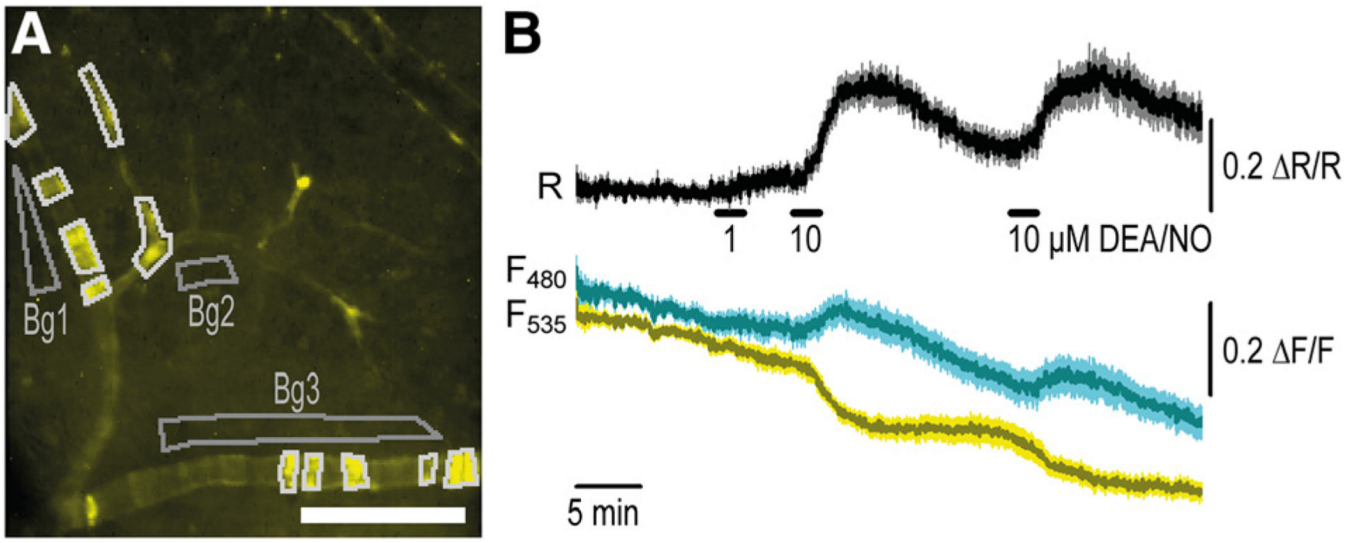

Figure 4. Cyclic GMP (cGMP) imaging in vessels of a retina acutely isolated from SM22-cGMP indicator with an EC_{50} of 500 nmol/L (cGi500) mice

A, Distribution of sensor fluorescence indicates mosaic expression in the vascular smooth muscle cells (VSMCs) of retinal vessels. **B**, On superfusion of 2-(N,N-diethylamino)-diazenolate-2-oxide diethylammonium salt (DEA/NO; 1 or 10 µmol/L), clear cGMP increases can be detected in these vessels. Responses of n=11 fluorescent regions outlined in white in **A** were measured, corrected with adjacent background regions (Bg1–3), and then averaged. Data shown are mean±SEM. Scale bar, 100 µm. Representative results from ≥4 experiments with independent tissue samples are shown.

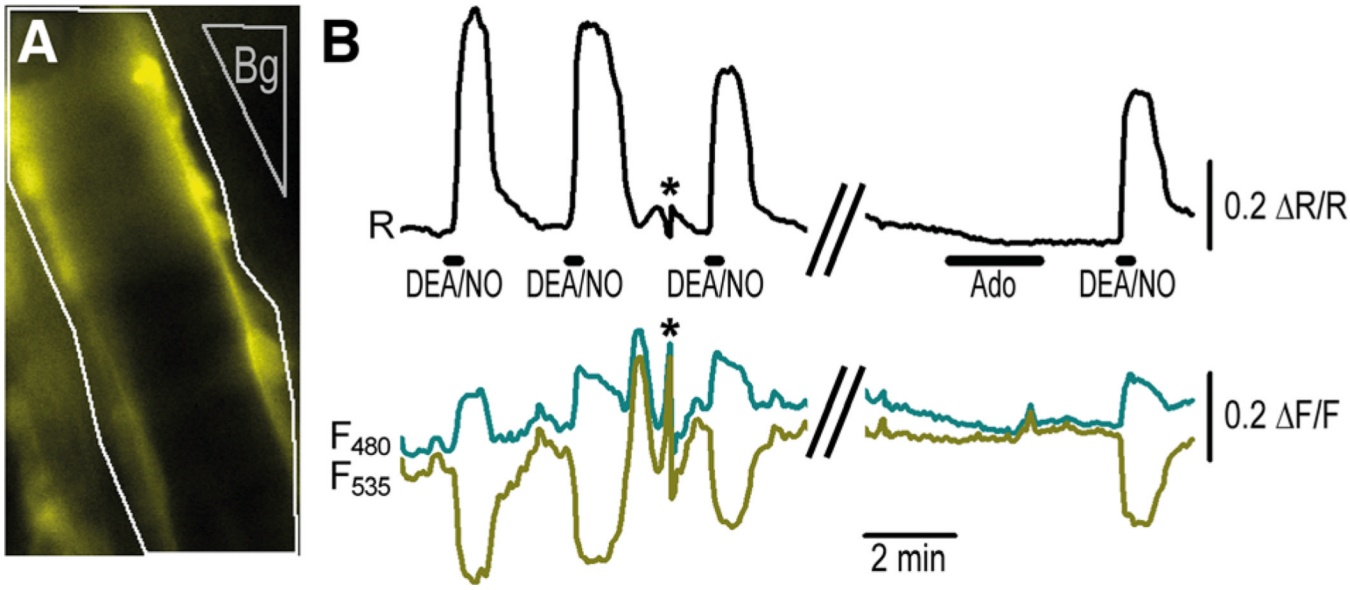

Figure 5. Cyclic GMP (cGMP) imaging in the cremaster microcirculation of an anesthetized R26-CAG-cGMP indicator with an EC_{50} of 500 nmol/L (cGi500)(L1) mouse

A,Distribution of fluorescence indicates strong cGi500 expression in vascular smooth muscle cells of cremaster arterioles. **B**, Robust cGMP transients can be detected in these vessels (outlined in white in **A**) on repeated superfusion with 2-(N,N-diethylamino)-diazenolate-2-oxide diethylammonium salt (DEA/NO; 10 μmol/L). Note that adenosine (Ado; 10 μmol/L), which is known to induce relaxation via the cAMP pathway, did not induce detectable ratio changes. Asterisks indicate artificial signal changes induced by focus drift. The region used for background correction of the fluorescence signals is indicated in **A** (Bg).

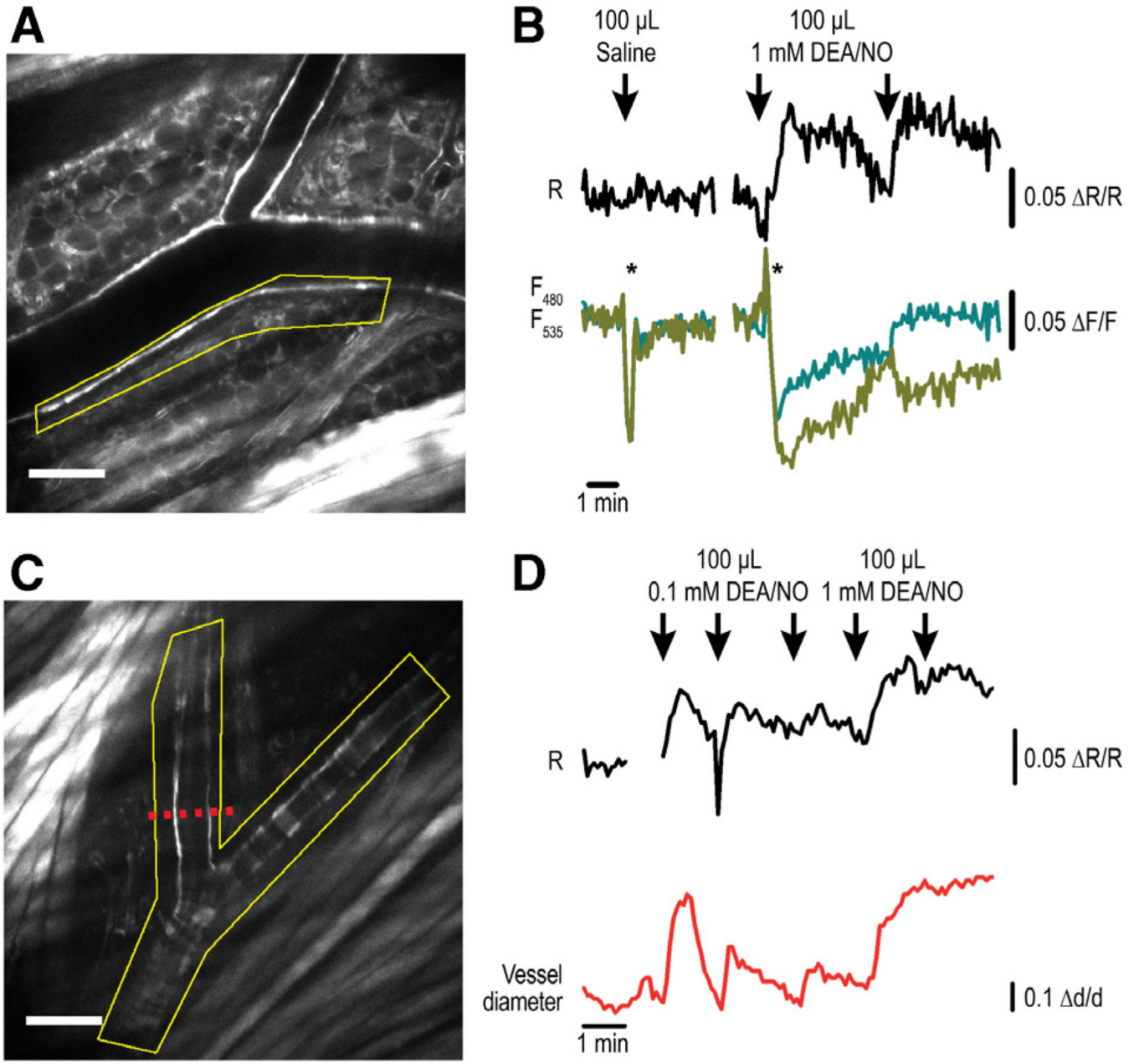

Figure 6. Detection of nitric oxide–induced vascular cyclic GMP (cGMP) signals associated with vasorelaxation in vivo in anesthetized R26-CAG-cGMP indicator with an EC_{50} of 500 nmol/L (cGi500)(L1) mice

Blood vessels in the skin were imaged in dorsal skinfold chambers by multiphoton fluorescence resonance energy transfer (FRET) microscopy. **A** and **C**, The distribution of sensor fluorescence (cyan fluorescent protein [CFP] channel) indicates strong expression in the skin, including the vasculature. Scale bars, 100 µm. **B**, cGMP imaging of the region outlined in **A** (yellow). Intravenous injection of 100 µL saline did not result in a FRET ratio change. Repeated injection of 100 µL of 1 mmol/L 2-(N,N-diethylamino)-diazenolate-2-oxide diethylammonium salt (DEA/NO) induced clear cGMP transients (black trace). Note that both saline and DEA/NO injection resulted in instantaneous alterations of CFP and yellow fluorescent protein (YFP) emissions (cyan and yellow traces) in the same direction

(indicated by asterisks). These changes barely affected the FRET ratio signal and were most likely artifacts induced by movements during the injection procedure. Only DEA/NO, not saline, resulted in sustained changes of CFP and YFP emission signals in opposite directions, indicative of cGMP binding to the sensor. **D**, cGMP imaging of the region outlined in **C** (yellow). Mice were injected intravenously 3 times with 100 μL of 0.1 mmol/L DEA/NO followed by 2 injections of 100 μL of 1 mmol/L DEA/NO. In parallel to the cGMP FRET signals (black trace), the vessel diameter (red trace) was measured at the location indicated by the red dashed line in **C**. Δd/d indicates relative diameter change.